On a spectral problem in magnetohydrodynamics and its relevance for the geodynamo

Stefani, F.; Tretter, C.;

Originally published:

October 2018

GAMM-Mitteilungen 41(2018)3, e201800012

DOI: https://doi.org/10.1002/gamm.201800012

GAMM-Mitteilungen, 16 October 2018

On a spectral problem in magnetohydrodynamics and its relevance for the geodynamo

Frank Stefani[1]* and **Christiane Tretter**[2,]**

[1] Helmholtz-Zentrum Dresden-Rossendorf, Bautzner Landstr. 400, 01328 Dresden, Germany
[2] Universität Bern, Mathematisches Institut (MAI), Sidlerstr. 5, 3012 Bern, Switzerland

Received XXXX, revised XXXX, accepted XXXX
Published online XXXX

Key words Magnetohydrodynamics, geodynamo, α^2 dynamo model, eigenvalue estimates
MSC (2000) 76W05, 86A25, 35Q86, 47A10, 47N50

One of the most remarkable features of the geodynamo is the irregular occurrence of magnetic field reversals. Starting with the operator theoretical treatment of a non-selfadjoint dynamo operator, we elaborate a dynamical picture of those reversals that rely on the existence of exceptional spectral points.

1 Introduction

Probably since more than 4 billion years, the liquid metal flow in the Earth's outer core has been working as a homogeneous, hydromagnetic dynamo that converts gravitational and thermal energy into magnetic field energy [1]. One of the most impressive features of the geomagnetic field is the irregular occurrence of polarity reversals, with a mean reversal rate of approximately 4-5 per Myr.

Recent numerical simulations of the coupled system of the Navier-Stokes equation for the velocity field and the induction equation for the magnetic field have been successful in reproducing not only the dominance of the axial dipole but also polarity reversals [2]. Reversals were also observed in one [3] of the recent liquid sodium dynamo experiments which have flourished during the last two decades [4]. However, neither in simulations nor in experiments it has been possible to accommodate all dimensionless parameters of the geodynamo [5].

A complementary approach to reversals investigates simplified, lower-dimensional models, with the underlying hope to capture the most essential characteristics of the reversal process. Perhaps the most simple reversal model of this kind was proposed by Pétrélis et al. [6] in form of the ordinary differential equation $\dot{\Theta} = a_1 + a_2 \sin(2\Theta) + \Delta\zeta(t)$, where Θ is related to the angle between the dipole and the quadrupole components of the field, and Δ is the amplitude of some noise. The dynamics of this system is governed by the existence of two pairs of stable and unstable fixed points, or a limit cycle for other parameters a_1 and a_2. Even below the saddle-node bifurcation, the noise term proportional to Δ can make the system run from

* E-mail: F.Stefani@hzdr.de
** Corresponding author E-mail: tretter@math.unibe.ch

one stable fixed point, via the nearest unstable fixed point, towards the opposite stable fixed point, thereby realizing a reversal.

Interestingly, this typical dynamical systems picture has an equivalent counterpart in the spectral theory of the dynamo operator that governs the magnetic field dynamics. The transitions between non-oscillatory and oscillatory eigenmodes, which are often observed here [7–11], are well-known in operator theory as spectral branch points – "exceptional points" of branching type of non-selfadjoint operators [12]. Such branch points are characterized not only by coalescing eigenvalues but also by a coalescence of two or more eigenvectors within a purely geometric eigenspace and the formation of a non-diagonal Jordan block structure with associated vectors [13, 14]. This is in contrast to "diabolical points" [15] which are points of an accidental crossing of two or more spectral branches with an unchanged diagonal block structure of the operator and without coalescing eigenvectors [12, 14].

In a series of papers [16–21], the magnetic field dynamics in the vicinity of an exceptional point was analyzed in greater detail numerically. For this purpose a so-called mean-field dynamo model of α^2 type was utilized, with a supposed spherically symmetric helical turbulence function α, which is, admittedly, far away from the reality of the Earth's dynamo. Remarkably, this simple model exhibited quite a number of the typical reversal features, in particular a temporal asymmetry with slow decay and fast recovery. However, since the eigenvalue problems underlying these time-evolutions are not symmetric, corresponding numerical computations are prone to be unreliable and thus have to be interpreted with care [22–24]. Moreover, there are questions that can never be answered by numerical computations, e.g. are there only finitely many non-real eigenvalues?

In the present paper, we will summarize and update this conceptual relation between the spectral theory of non-selfadjoint dynamo operators and the theory of geodynamo reversals. After a short general introduction into dynamo theory, we will streamline the operator-theoretical treatment of spherically symmetric α^2 dynamos, as elaborated in [25, 26], with focus on some strict global estimates for the eigenvalues of these operators, including an anti-dynamo theorem and a result on the finiteness of the number of non-real eigenvalues. Then we will move on to the temporal magnetic field evolution, which takes into account the dynamical back-reaction of the magnetic field on the source of its generation (i.e. α). Here we will show how the various features of geodynamo reversals trace back to the spectral theory of the underlying operators. The paper will close with an outlook on future developments.

2 Theoretical basis of dynamo theory

Dynamo theory starts with Ampère's law, Faraday's law, and Ohm's law in electrical conductors moving with velocity $\mathbf{v}$,

$$\nabla \times \mathbf{B} = \mu_0 \mathbf{j} \,, \tag{1}$$

$$\nabla \times \mathbf{E} = -\dot{\mathbf{B}} \,, \tag{2}$$

$$\mathbf{j} = \sigma(\mathbf{E} + \mathbf{v} \times \mathbf{B}) \,, \tag{3}$$

where σ denotes the conductivity of the fluid and μ_0 is the permeability of the vacuum (we suppose all materials to be non-magnetic). We have skipped the displacement current in Eq. (1) since the quasi-stationary approximation is usually fulfilled in good conductors. Taking

the $curl$ of Eqs. (1) and (3), and inserting into Eq. (2), one readily arrives at the compact *induction equation* for the magnetic field,

$$\frac{\partial \mathbf{B}}{\partial t} = \nabla \times (\mathbf{v} \times \mathbf{B}) + \frac{1}{\mu_0 \sigma} \Delta \mathbf{B} \; . \tag{4}$$

In deriving Eq. (4) we have assumed, for simplicity, σ and μ to be constant in the considered region (generalizations can be found in [27]), and we have exploited the fact that the magnetic field is source-free,

$$\nabla \cdot \mathbf{B} = 0 \; . \tag{5}$$

Assuming that there are no excitations of the magnetic field from outside, i.e. the field is being *self-excited* by the dynamo process, the boundary condition becomes

$$\mathbf{B} = \mathbf{O}(r^{-3}) \quad \text{as} \quad r \to \infty \; . \tag{6}$$

Obviously, the evolution of the magnetic field in Eq. (4) is governed by the competition between generation and diffusion of the field. For vanishing velocity the magnetic field will disappear within a typical decay time $t_d = \mu_0 \sigma l^2$, with l being a typical length scale of the system. When switched on, the advection by the velocity field $\mathbf{v}$ can lead to an increase of $\mathbf{B}$ within a kinematic time $t_k = l/v$, where v is a typical velocity scale. If this kinematic time becomes smaller than the diffusion time, the net effect of the evolution can become positive, leading to a growing magnetic field. Comparing the diffusion time-scale with the kinematic time-scale, we get a dimensionless number that governs the "fate" of the magnetic field. This number is called the magnetic Reynolds number R_m,

$$R_m = \mu_0 \sigma l v \; . \tag{7}$$

Depending on the specific flow pattern, the critical values of R_m for dynamo action to set in are typically in the range of 10^1 to 10^3.

An important feature of dynamo theory concerns the assumptions on the velocity field. If we assume the velocity to be steady, the time dependence of $\mathbf{B}$ in Eq. (4) becomes exponential according to $\mathbf{B}(\mathbf{r}, t) = \exp(\lambda t)\hat{\mathbf{B}}(\mathbf{r})$, and the corresponding *kinematic* dynamo problem can be rewritten as a time-independent eigenvalue equation. The eigenvalue parameter $\lambda = p + 2\pi \mathrm{i} f$ is complex, with growth rate p and frequency f. The onset of dynamo action occurs for $\mathrm{Re}\,\lambda = p \geq 0$. However, according to Lenz's rule, the velocity field being the source of dynamo action cannot remain unaffected when the magnetic field grows. The increasing magnetic field induces an increasing Lorentz force $\mathbf{j} \times \mathbf{B}$ which acts back on the velocity field. In general, the evolution of the velocity field is governed by the Navier-Stokes equation

$$\frac{\partial \mathbf{v}}{\partial t} + (\mathbf{v} \cdot \nabla)\mathbf{v} = -\frac{\nabla p}{\rho} + \frac{1}{\mu_0 \rho}(\nabla \times \mathbf{B}) \times \mathbf{B} + \nu \Delta \mathbf{v} + \mathbf{f}_d \; , \tag{8}$$

where ρ and ν denote the density and the kinematic viscosity of the fluid, respectively, p is the pressure, and $\mathbf{f}_d$ symbolizes driving forces. The Lorentz force in Eq. (8) puts Lenz's rule into action: the magnetic field acts back on the flow, in general weakening the source of its own generation. The treatment of the coupled system of Eqs. (4) and (8), which is called the *dynamically consistent* dynamo problem, is much more intriguing than the treatment of the linear induction equation alone.

A second characteristic feature is whether or not the turbulent character of practically all dynamo related flows is reflected by the dynamo model. *Laminar models* are described by the unchanged Eq. (4) with neglected turbulence. The self-excited magnetic field varies on the same length scale as the velocity field does. *Mean-field dynamo models*, on the other hand, are relevant for highly turbulent flows. In this case the velocity and the magnetic field are considered as superpositions of mean and fluctuating parts, $\mathbf{v} = \overline{\mathbf{v}} + \mathbf{v}'$ and $\mathbf{B} = \overline{\mathbf{B}} + \mathbf{B}'$. From Eq. (4) we obtain the equation for the mean part $\overline{\mathbf{B}}$,

$$\frac{\partial \overline{\mathbf{B}}}{\partial t} = \nabla \times (\overline{\mathbf{v}} \times \overline{\mathbf{B}} + \mathcal{E}) + \frac{1}{\mu_0 \sigma} \Delta \overline{\mathbf{B}} \; . \tag{9}$$

Obviously, the equation for the mean-field is identical to the equation for the original field, except for one additional term

$$\mathcal{E} = \overline{\mathbf{v}' \times \mathbf{B}'} \; , \tag{10}$$

which represents the mean electromagnetic force (emf) due to the correlated fluctuations of the velocity and the magnetic field. The elaboration of mean-field dynamo models by Steenbeck, Krause and Rädler [28] in the sixties was a breakthrough in dynamo theory. They showed that the mean electromotive force in a non-mirrorsymmetric turbulence typically is of the form

$$\mathcal{E} = \alpha \overline{\mathbf{B}} - \beta \nabla \times \overline{\mathbf{B}} \; , \tag{11}$$

with a parameter function α that is non-zero for helical turbulence and a parameter β that describes the enhancement of the electrical resistivity due to turbulence. The effect that helical fluid motion can induce an electromotive force that is *parallel* to the magnetic field is now commonly known as the α-effect. Dynamo models based on the α-effect have played an enormous role in the study of solar and galactic magnetic fields, and we will restrict all following considerations to a model of this kind.

Specifically, we will be concerned with the most simple form of mean-field dynamos in spherical geometry assuming a spherical symmetry of the helical turbulence parameter, i.e. $\alpha(\mathbf{r}) = \alpha(r)$, $r \in [0,1]$. Although this is physically not realistic (for the geodynamo, one would find a pronounced North-South asymmetry of α), the model is both simple enough for (quasi-) analytical treatments and complex enough for allowing non-trivial back-reaction effects.

In spherical geometry, we can decompose $\mathbf{B}$ into a poloidal and a toroidal field component according to $\mathbf{B} = -\nabla \times (\mathbf{r} \times \nabla \mathcal{S}) - \mathbf{r} \times \nabla \mathcal{T}$. The defining scalar functions $\mathcal{S}$ and $\mathcal{T}$ are then expanded in spherical harmonics of degree l and order m with expansion coefficients $s_{l,m}(r,t)$ and $t_{l,m}(r,t)$. For the spherically symmetric case $\alpha(\mathbf{r}) = \alpha(r)$ considered here, the induction equation decouples for each l and m into the pair of equations

$$\frac{\partial s_l}{\partial t} = \frac{1}{r} \frac{d^2}{dr^2}(r s_l) - \frac{l(l+1)}{r^2} s_l + \alpha(r,t) t_l \; , \tag{12}$$

$$\frac{\partial t_l}{\partial t} = \frac{1}{r} \frac{d}{dr} \left[\frac{d}{dr}(r t_l) - \alpha(r,t) \frac{d}{dr}(r s_l) \right] - \frac{l(l+1)}{r^2} [t_l - \alpha(r,t) s_l] \; , \tag{13}$$

where the length is measured in units of the outer radius R, the time in units of $\mu_0 \sigma R^2$, and α in units of $(\mu_0 \sigma R)^{-1}$. The boundary conditions are given by

$$\partial s_l / \partial r|_{r=1} + (l+1) s_l(1) = t_l(1) = 0 \; . \tag{14}$$

The absence of the order m in Eqs. (12), (13) follows from the spherical symmetry of α. It implies, in particular, a complete degeneracy of axial and equatorial dipole modes. It is clear that for any more realistic model (e.g. with inclusion of the North-South asymmetry of α) this degeneration would be lifted.

3 Spectral theory of a spherically symmetric α^2 dynamo

In this section, we focus on the spectral theory of spherically symmetric α^2 dynamos. Assuming $\alpha(\mathbf{r}) = \alpha(r)$ as time-independent, and substituting $y_1 = rs_l$ and $y_2 = rt_l$, we rewrite the time evolution equation system (12), (13), (14) in the previous section as an eigenvalue problem for a pair of coupled linear ordinary differential equations, indexed by the degree $l \in \mathbb{N} = \{1, 2, \dots\}$ of the spherical harmonics,

$$\begin{pmatrix} \partial_r^2 - \dfrac{l(l+1)}{r^2} & \alpha(r) \\ -\partial_r \alpha(r) \partial_r + \alpha(r) \dfrac{l(l+1)}{r^2} & \partial_r^2 - \dfrac{l(l+1)}{r^2} \end{pmatrix} \begin{pmatrix} y_1 \\ y_2 \end{pmatrix} = \lambda \begin{pmatrix} y_1 \\ y_2 \end{pmatrix}, \quad r \in (0,1] \,, \tag{15}$$

in the product space $L_2(0,1) \oplus L_2(0,1)$ subject to the boundary condition

$$\begin{pmatrix} (\partial_r + l) y_1 \\ y_2 \end{pmatrix} (1) = 0 \,. \tag{16}$$

In the following, for brevity, we call the eigenvalue problem (15), (16) dynamo problem.

In view of the time separation ansatz $\mathbf{B}(\mathbf{r}, t) = \exp(\lambda t) \hat{\mathbf{B}}(\mathbf{r})$ of the corresponding magnetic field modes, one naturally distinguishes between decaying or subcritical modes ($\mathrm{Re}\,\lambda < 0$) and amplifying or supercritical modes ($\mathrm{Re}\,\lambda > 0$), as well as between oscillatory modes ($\mathrm{Im}\,\lambda \neq 0$) and non-oscillatory modes ($\mathrm{Im}\,\lambda = 0$). The physically relevant self-sustaining dynamo configurations are mainly defined by a few supercritical modes, whereas possible polarity reversals of the magnetic fields are closely related to the existence of oscillatory modes close to criticality ($\mathrm{Re}\,\lambda \approx 0$, $\mathrm{Im}\,\lambda \neq 0$) (see [17], [18]).

The dynamo problem (15), (16) is not symmetric, and hence not selfadjoint, because the differential expressions in the off-diagonal corners of (15) are not formally adjoint to each other, they even do not have the same orders. Therefore reliable information on the true eigenvalues of (15), (16) is very hard to obtain since it is well-known that numerical eigenvalue approximations for non-selfadjoint problems are prone to two undesirable effects (see e.g. [23]). The first such effect is spectral pollution, i.e. eigenvalue approximations may converge to a limiting point that is not a true eigenvalue, a so-called spurious eigenvalue. The second undesirable effect is failure of spectral inclusion, i.e. a true eigenvalue may not be approximated. Both effects are particularly unwanted here: a spurious eigenvalue in the half-plane $\mathrm{Re}\,\lambda > 0$ could wrongly predict the existence of supercritical modes and hence of a dynamo effect, while failure of spectral inclusion for a true eigenvalue in the half-plane $\mathrm{Re}\,\lambda > 0$ might miss to predict the existence of a dynamo effect.

In view of this, there is an urgent need for guaranteed analytical information on the spectrum of the dynamo problem (15), (16) in terms of the helical turbulence function α. A valuable tool to obtain reliable information on the location of eigenvalues of non-selfadjoint

problems is perturbation theory for linear operators. In the simplest case, assume that T is a selfadjoint (or normal) unbounded operator in a Hilbert space H with domain $D(T)$ and S is a bounded operator in H. Then we know that the spectrum of T is real, $\sigma(T) \subset \mathbb{R}$, and the resolvent norm of T satisfies

$$\|(T-\lambda)^{-1}\| = \frac{1}{\operatorname{dist}(\lambda, \sigma(T))}\,, \quad \lambda \notin \sigma(T)\,, \tag{17}$$

(see [12, Thm. V.3.2]). Hence a Neumann series argument (see [12, Ex. I.4.5]) shows that for

$$T+S-\lambda = (I_H + S(T-\lambda)^{-1})(T-\lambda)\,, \quad \lambda \notin \sigma(T)\,, \tag{18}$$

the left hand side is bijective, and hence $\lambda \notin \sigma(T+S)$, provided that $\|S(T-\lambda)^{-1}\| < 1$. The latter is satisfied if $\|S\|\|(T-\lambda)^{-1}\| = \|S\|/\operatorname{dist}(\lambda, \sigma(T)) < 1$ and so we obtain that the spectrum of the perturbed operator $T+S$ satisfies the inclusion

$$\sigma(T+S) \subset \sigma(T) + \|S\| = \{\lambda \in \mathbb{C} : \operatorname{dist}(\lambda, \sigma(T)) \le \|S\|\}\,. \tag{19}$$

If, however, T is no longer selfadjoint (but closed, i.e. T has closed graph), then the resolvent norm can no longer be controlled in terms of the distance to the spectrum, but only in terms of the distance to the numerical range $W(T) := \{(Tx, x) : x \in D(T), \|x\| = 1\}$ of T,

$$\|(T-\lambda)^{-1}\| \le \frac{1}{\operatorname{dist}(\lambda, W(T))}\,, \quad \lambda \notin \overline{W(T)}\,. \tag{20}$$

Note that this effect already appears in finite dimensions, the simplest example being a linear operator given by the Jordan block matrix

$$A = \begin{pmatrix} 0 & 1 \\ 0 & 0 \end{pmatrix}, \quad (A-\lambda)^{-1} = \begin{pmatrix} -\lambda^{-1} & -\lambda^{-2} \\ 0 & -\lambda^{-1} \end{pmatrix}, \ \lambda \notin \sigma(A) = \{0\}\,,$$

for which $W(A) = K_{1/2}(0) = \{z \in \mathbb{C} : |z| \le 1/2\}$. Clearly, the resolvent norm of A does not behave like $1/\operatorname{dist}(\lambda, \sigma(A)) = |\lambda|^{-1}$ as $\lambda \to 0$.

The consequence of the different resolvent norm bounds in (17) and (20) is that the spectrum of the perturbed operator $T+S$ now satisfies the inclusion

$$\sigma(T+S) \subset W(T) + \|S\| = \{\lambda \in \mathbb{C} : \operatorname{dist}(\lambda, W(T)) \le \|S\|\}\,. \tag{21}$$

Thus the relation to the spectrum $\sigma(T)$ of the unperturbed operator T is lost if T is not self-adjoint!

Both spectral enclosures (19), (21) may be generalized to perturbations S defined on some domain $D(S) \subset H$ that are no longer bounded, but only relatively bounded with respect to T or T-bounded [29]. This means that $D(T) \subset D(S)$ and there exist constants $a, b \ge 0$ with

$$\|Sx\| \le a\|x\| + b\|Tx\|\,, \quad x \in D(T)\,; \tag{22}$$

the infimum δ_T of all $b \ge 0$ such that (22) holds for some $a \ge 0$ is called the T-bound of S (see [12, Sect. IV.1]). Note that if S is bounded, it is T-bounded with T-bound 0 since we can choose $a = \|S\|$ and $b = 0$ in (22) and that otherwise (22) need not hold with $b = \delta_T$.

For the dynamo problem (15), (16) these perturbation results can be applied in different ways, depending on the choice of the unperturbed operator, to obtain rigorous and analytic enclosures of the spectrum via (19) or (21), respectively. To this end, we first have to cast (15), (16) into a suitable operator framework.

In the Hilbert space $L_2(0,1)$ we consider the Bessel and Bessel type differential expressions, respectively,

$$\tau_l := -\partial_r^2 + \frac{l(l+1)}{r^2}\,, \quad \tau_{l,\alpha} := -\partial_r \alpha(r) \partial_r + \alpha(r) \frac{l(l+1)}{r^2}\,, \quad \partial_r := \frac{\mathrm{d}}{\mathrm{d}r}\,, \tag{23}$$

occurring in (15) where $l \in \mathbb{N} = \{1, 2, \dots\}$ is fixed and $\alpha : [0,1] \to \mathbb{R}$ is assumed to be a continuously differentiable real-valued function, $\alpha \in C^1([0,1], \mathbb{R})$. We introduce the two Bessel differential operators $A_{l,l}$, $A_{l,\infty}$ and the Bessel type differential operator $A_{l,\alpha,\infty}$ in $L_2(0,1)$ by

$$\begin{aligned} A_{l,l} x &= \tau_l x\,, \quad x'(1) + l x(1) = 0\,, \qquad \text{and} \qquad A_{l,\infty} x = \tau_l x\,, \quad x(1) = 0\,, \\ A_{l,\alpha,l} x &= \tau_{l,\alpha} x\,, \quad x'(1) + l x(1) = 0\,, \end{aligned}$$

on respective domains $D(A_{l,l})$, $D(A_{l,\infty})$ and $D(A_{l,\alpha,\infty})$ (see [26, Sect. 2] for details). Then the dynamo problem (15), (16) can be written as an eigenvalue problem

$$(\mathbf{A}_l - \lambda) y = 0\,, \quad y \in D(\mathbf{A}_l)\,,$$

for the operator matrix $\mathbf{A}_l$ in the product Hilbert space $L_2(0,1) \oplus L_2(0,1)$ given by

$$\mathbf{A}_l := \begin{pmatrix} -A_{l,l} & \alpha \\ A_{l,\alpha,l} & -A_{l,\infty} \end{pmatrix}, \quad D(\mathbf{A}_l) := D(A_{l,l}) \oplus D(A_{l,\infty})\,. \tag{24}$$

In general, the spectrum of a differential operator matrix need not be discrete even if this is true for all its entries, e.g. if the product of the orders on the diagonal and the product of the orders in the off-diagonal corners are the same (see e.g. [30, Sect. 2.4], [31, Sect. 3.1]). Here this does not happen, the spectrum of the operator matrix $\mathbf{A}_l$ remains discrete, i.e. it consists only of countably many eigenvalues of finite algebraic multiplicity without finite accumulation point.

The first decomposition of the operator matrix $\mathbf{A}_l$ one might think of is to split off the right upper entry,

$$\mathbf{A}_l = \begin{pmatrix} -A_{l,l} & 0 \\ A_{l,\alpha,l} & -A_{l,\infty} \end{pmatrix} + \begin{pmatrix} 0 & \alpha \\ 0 & 0 \end{pmatrix} =: T_1 + S_1\,. \tag{25}$$

The advantage of this splitting is that the operator S_1, whose only non-zero entry is the multiplication operator by the function α, is bounded and that the spectrum of the unperturbed operator T_1 is known, $\sigma(T_1) = \sigma(-A_{l,l}) \cup \sigma(-A_{l,\infty}) \subset (-\infty, 0)$, being the union of the eigenvalues of the diagonal entries, which are the zeros of certain Bessel functions of fractional order. The disadvantage is that the unperturbed operator T_1 is *not* selfadjoint (nor normal) and so we *cannot* conclude that the spectrum of $\mathbf{A}_l$ lies in a $\|S_1\|$-neighbourhood of the eigenvalues of $-A_{l,l}$ and $-A_{l,\infty}$, and only the spectral inclusion (21) would apply.

However, using the operator matrix structure of T_1 and S_1, we can obtain a tighter spectral enclosure. Indeed, rather than estimating the norm product $\|S_1\|\|(T_1-\lambda)^{-1}\|$, we compute the product $S_1(T_1-\lambda)^{-1}$ (comp. (18)) and use that it only has two non-zero entries to obtain

$$I + S_1(T_1-\lambda)^{-1} = \begin{pmatrix} I - \alpha(A_{l,\infty}+\lambda)^{-1}A_{l,\alpha,l}(A_{l,l}+\lambda)^{-1} & -\alpha(A_{l,\infty}+\lambda)^{-1} \\ 0 & I \end{pmatrix}$$

for $\lambda \notin \sigma(-A_{l,l}) \cup \sigma(-A_{l,\infty})$. Using the relation

$$A_{l,\alpha,l}x = \alpha A_{l,l}x - \alpha' \partial_r x \ , \quad x \in D(A_{l,l}) = D(A_{l,\alpha,l}) \ , \tag{26}$$

together with the resolvent estimate (17) for the selfadjoint operators $A_{l,l}$, $A_{l,\infty}$ and the estimate $\|\partial_r A_{l,l}^{-1/2}\| \le 1$, one can derive the following result on the non-existence of eigenvalues of the dynamo operator $\mathbf{A}_l$, and hence of the dynamo problem (15), (16) (see [26, Thm. 4.6 and Cor. 4.8]).

Here, for a continuous function $f \in C([0,1],\mathbb{C})$ we denote by $\|f\|_\infty := \max_{r\in[0,1]} |f(r)|$ its maximum norm.

Anti-dynamo theorem. *The dynamo operator $\mathbf{A}_l$ associated with the α^2 dynamo problem* (15), (16) *possesses no eigenvalues with real part > 0 if $\alpha \in C^1([0,1],\mathbb{R})$ and*

$$\|\alpha\|_\infty^2 + \frac{\|\alpha\|_\infty^2 \|\alpha'\|_\infty^2}{j_{l-\frac12,1}} < j_{l+\frac12,1}^2 \tag{27}$$

where $j_{l-\frac12,1}$ and $j_{l+\frac12,1}$ are the smallest non-zero zeros of the two Bessel functions $J_{l-\frac12}$ and $J_{l+\frac12}$, respectively. The full dynamo operator $\mathbf{A} = \bigoplus_{l=1}^\infty \mathbf{A}_l$ possesses no eigenvalues with real part > 0 if (27) *holds for $l = 1$.*

Note that the last claim follows from the interlacing property $j_{l-\frac12,1} < j_{l+\frac12,1}$ of the Bessel zeros for $l \in \mathbb{N}$ (see [32, 9.5.2 and 10.1]) which implies that $j_{\frac12,1} \le j_{l-\frac12,1}$ and $j_{\frac32,1} \le j_{l+\frac12,1}$ for $l \in \mathbb{N}$.

Example 1. For the simplest profile $\alpha_{kin}(r) = C$, $r \in [0,1]$, the eigenvalue problem (15), (16) is analytically solvable (see e.g. [28]) to give, for $l = 1$, a critical value of $C = j_{\frac32,1}$ (~ 4.493409). In this particular case, our general anti-dynamo criterion (27) specializes to

$$\|\alpha\|_\infty^2 = C^2 < j_{\frac32,1}^2 \ (\sim 4.493409^2) \ ,$$

which perfectly matches the analytically known critical value for C and shows that (27) is sharp in this case.

Example 2. For the kinematic profile $\alpha_{kin}(r) = 1.916 \cdot C \cdot (1 - 6\ r^2 + 5\ r^4)$, $r \in [0,1]$ (which will serve as a paradigmatic profile for the reversal studies in the next section), it is not difficult to check that

$$\|\alpha\|_\infty = \alpha(0) = 1.916 \cdot C \ , \quad \|\alpha'\|_\infty = \alpha'(1) = 8 \cdot 1.916 \cdot C \ .$$

The Bessel zeros in (27) for $l = 1$ satisfy $j_{\frac12,1} = \pi \le 3.142$ and $j_{\frac32,1} \le 4.494$, respectively, and so (27) for $l = 1$ holds if

$$1.916^2 \cdot C^2 \Big(1 + \frac{8}{3.142}\Big) < 4.494^2 \, .$$

Hence it is analytically guaranteed that for α_{kin} with $C < 1.725$ the dynamo problem (15), (16) possesses no eigenvalues with real part > 0 for any $l \in \mathbb{N}$.

While the above decomposition (25) shows, more generally, that all eigenvalues lie in a half-plane $\operatorname{Re}\lambda \le a_l$ with some constant $a_l \in \mathbb{R}$ and provide good control of the real parts of all eigenvalues, it does not provide a good estimate for the imaginary parts. In fact, it only yields an estimate of the form $|\operatorname{Im}\lambda| \le h_l(\operatorname{Re}\lambda)$ for $\operatorname{Re}\lambda \in (-\infty, a_l]$ with a continuous strictly decreasing function $h_l : (-\infty, a_l] \to [0,\infty)$ with $h_l(a_l) = 0$, but $\lim_{t\to-\infty} h_l(t) = \infty$ and $\lim_{t\nearrow a_l} h_l'(t) = -\infty$. So in particular, it does not exclude that the imaginary parts of the eigenvalues tend to $\pm\infty$ when their real parts tend to $-\infty$.

In order to obtain a better estimate for the imaginary parts of the eigenvalues, and possibly information on the number of non-real eigenvalues, a more subtle decomposition of the dynamo operator $\mathbf{A}_l$ is needed, preceded by a quasi-similarity transformation with the (unbounded) operator matrix

$$\mathcal{W} := \begin{pmatrix} A_{l,l}^{1/2} & 0 \\ 0 & I \end{pmatrix}, \quad D(\mathcal{W}) := D(A_{l,l}^{1/2}) \oplus L_2(0,1) \,.$$

Although the transformation is not bounded, the spectra of $\mathbf{A}_l$ and of the transformed operator $\mathcal{W}^{-1}\mathbf{A}_l\mathcal{W}$ coincide since they consist only of eigenvalues. Invoking the relation (26) again, we see that

$$\mathcal{W}^{-1}\mathbf{A}_l\mathcal{W} = \begin{pmatrix} -A_{l,l} & A_{l,l}^{1/2}\alpha \\ \alpha A_{l,l}^{1/2} & -A_{l,\infty} \end{pmatrix} + \begin{pmatrix} 0 & 0 \\ -\alpha'\partial_r A_{l,l}^{-1/2} & 0 \end{pmatrix} =: T_2 + S_2 \,. \tag{28}$$

The advantage of this decomposition is that here the unperturbed operator T_2 is selfadjoint and at the same time the perturbation S_2 is bounded (since $\|\partial_r A_{l,l}^{-1/2}\| \le 1$) with $\|S_2\| \le \|\alpha'\|_\infty$; by (19) this immediately implies that the imaginary parts of all eigenvalues of the dynamo operator $\mathbf{A}_l$ are uniformly bounded by $\|\alpha'\|$,

$$|\operatorname{Im}\lambda| \le \|\alpha'\|_\infty \quad \text{for all } \lambda \in \sigma(\mathbf{A}_l) \,; \tag{29}$$

note that (29) readily yields that for constant α all eigenvalues of the dynamo problem (15), (16) are real.

The disadvantage of the decomposition (28) is that we no longer have explicit information on the spectrum of the unperturbed operator T_2. Nevertheless, T_2 is a *diagonally dominant* operator matrix (see [30, Def. 2.2.1]) and we can decompose the operator T_2 into its dominating diagonal and the off-diagonal part,

$$T_2 = \begin{pmatrix} -A_{l,l} & 0 \\ 0 & -A_{l,\infty} \end{pmatrix} + \begin{pmatrix} 0 & A_{l,l}^{1/2}\alpha \\ \alpha A_{l,l}^{1/2} & 0 \end{pmatrix} =: D_2 + O_2 \,.$$

Here both the diagonal part D_2 and the off-diagonal part O_2 are selfadjoint and the spectrum $\sigma(D_2) = \sigma(-A_{l,l}) \cup \sigma(-A_{l,\infty})$ is given by the two interlacing sequences of non-zero Bessel zeros $-\lambda_k(l,l) = -j_{l-\frac12,k}^2$ of $\lambda \mapsto J_{l-\frac12}(\sqrt{\lambda})$ and $-\lambda_k(l,\infty) = -j_{l+\frac12,k}^2$ of $\lambda \mapsto J_{l+\frac12}(\sqrt{\lambda})$, respectively, for $k \in \mathbb{N}$,

$$\sigma(D_2) = \{-\lambda_k(l,l)\}_{k=1}^\infty \cup \{-\lambda_k(l,\infty)\}_{k=1}^\infty = \{-j_{l-\frac12,k}^2\}_{k=1}^\infty \cup \{-j_{l+\frac12,k}^2\}_{k=1}^\infty \,, \tag{30}$$

and all eigenvalues of D_2 are simple. Further, it can be shown that the off-diagonal part O_2 is D_2-bounded and constants a_α, $b_\alpha \geq 0$ in the respective inequality (22) may be found explicitly in terms of the helical turbulence function α. Applying a more advanced perturbation result (see [29, Thm. 2.1]), one can establish estimates for the eigenvalues of T_2 which guarantee that the eigenvalues $\{\mu_k(t)\}_{k=1}^{\infty}$ of the selfadjoint operator $D_2 + tO_2$ for $t \in [0,1]$ vary in intervals around the eigenvalues of D_2 that remain disjoint for all $t \in [0,1]$. In particular, this guarantees that the eigenvalues $\{\mu_k(1)\}_{k=1}^{\infty}$ of $T_2 = D_2 + O_2$ are still all simple. Moreover, after some tedious and clever analysis, one can estimate their differences to the eigenvalues of D_2, i.e. the Bessel zeros in (30) in terms of the relative boundedness constants a_α, $b_\alpha \geq 0$.

These involved eigenvalue estimates may be combined with the asymptotics of the Bessel zeros forming the spectrum of D_2, and with the following operator theoretic property. Since the helical turbulence function α is real-valued, the eigenvalues of the dynamo operator $\mathbf{A}_l$, and hence of the operator $T_2 + S_2$ in (28) are symmetric to the real axis. If it is guaranteed that the eigenvalues of the selfadjoint operator T_2 are all simple, then after the perturbation S_2 eigenvalues may only become complex (and hence form a complex conjugate pair) if two eigenvalues coalesce (comp. [33]). The eigenvalue estimates for T_2 together with the fact that S_2 is bounded finally yield the following result (see [34, Thm. 3.13]).

Theorem. *If $\alpha \in C^2([0,1],\mathbb{R})$ and $\|\alpha\|_\infty < \pi/2^{5/4}$, then the dynamo problem* (15), (16) *has at most a finite number of non-real* (*complex conjugate pairs of*) *eigenvalues.*

We mention that the norm bound on α guarantees the simplicity of the eigenvalues of T_2, so we expect it is neither sharp nor even necessary; e.g. for the kinematic profile $\alpha_{kin}(r) = 1.916 \cdot C \cdot (1 - 6\ r^2 + 5\ r^4)$, $r \in [0,1]$, the bound is satisfied if $C < 0.689$. Note also that the derivative α' will play a role if one is interested in estimating the number of non-real eigenvalue pairs (it is zero if $\alpha' = 0$, i.e. if α is constant).

It should be emphasized that it is *not* possible to obtain a result on the finiteness of the number of non-real eigenvalues by means of numerical computations, simply because - even if they were guaranteed computations e.g. with interval arithmetic (see [35, 36]) - they can only cover bounded regions of the complex plane in finite time.

4 A simplified reversal model for the geodynamo

In the previous section we have seen that spherically symmetric α^2 dynamos may have complex eigenvalues as long as the radial profile $\alpha(r)$ is not too simple (e.g. for constant α there are only real eigenvalues). Now we assume that the profile $\alpha(r)$ in the kinematic regime, $\alpha_{kin}(r)$, leads to dynamo action which might be either of non-oscillatory or oscillatory type. After self-excitation, i.e. exponential magnetic field growth, has set in, saturation is ensured by a reduction, or "quenching", of α. This effect can be interpreted as a realization of Lenz's rule, according to which the magnetic field acts against the source of its own generation.

Actually, this quenching is a non-trivial and strongly debated mechanism. In order to remain within the framework of spherically symmetric α^2 dynamos, we take resort to the simplification that the quenching of the α profile is affected by the angularly averaged magnetic field energy which can be expressed in terms of $s(r,t)$ and $t(r,t)$. Of course, a realistic quenching would introduce terms breaking the spherical symmetry of α.

In addition to the quenching effect, we will later consider the α profile to be further affected by some noise terms which are supposed to be constant within a correlation time τ_{corr}.

Physically, this noise could be understood as a consequence of changing boundary conditions for the core flow, but also as a substitute for the omitted influence of higher multipole modes on the dominant dipole mode.

Putting these two effects together, the α profile takes on the time dependent form

$$\alpha(r,t) = C\,\frac{\alpha_{kin}(r)}{1+E_{mag}(r,t)/E^0_{mag}} + \Xi(r,t)\ , \tag{31}$$

where E_{mag} is the magnetic energy, averaged over the angles,

$$E_{mag}(r,t) = \frac{2s_1^2(r,1)}{r^2} + \frac{1}{r^2}\left(\frac{\partial(rs_1(r,t))}{\partial r}\right)^2 + t_1^2(r,t)\ . \tag{32}$$

In the numerical scheme, the noise term $\Xi(r,t)$ will be treated in form of a Taylor expansion,

$$\Xi(r,t) = \xi_1(t) + \xi_2(t)\ r^2 + \xi_3(t)\ r^3 + \xi_4(t)\ r^4\ , \tag{33}$$

with the noise correlation given by $\langle \xi_i(t)\xi_j(t+t_1)\rangle = D^2(1-|t_1|/\tau_{corr})\Theta(1-|t_1|/\tau_{corr})\delta_{ij}$.

In summary, our model is governed by four parameters: the magnetic Reynolds number C, the noise amplitude D, the noise correlation time τ_{corr}, and the mean magnetic energy E^0_{mag} in the saturated regime.

The system of equations (12), (13) and (31) is time-stepped using an Adams-Bashforth method. For the following examples, the correlation time τ_{corr} has been set to 0.02, and E^0_{mag} has been chosen to be 100. The details of these choices are not very relevant. Roughly speaking, a shorter correlation time τ_{corr} would require a stronger noise amplitude D in order to yield the same effect.

In the remainder of this section, we analyze in detail a dynamo which starts from the kinematic profile $\alpha_{kin}(r) = 1.916 \cdot C \cdot (1 - 6\ r^2 + 5\ r^4)$, $r \in [0,1]$, (the prefactor 1.916 merely serves for normalizing the profile's intensity to 1). This profile α_{kin}, with its sign change along the radius (see the full line in Fig. 1 (b)), is a good candidate to exhibit complex eigenvalues and, therefore, an oscillatory dynamo behaviour. Indeed, the dynamo (upper panel of Fig. 1 (a)) arising at $C = 6.8$, which is only slightly larger than the critical value of 6.78, turns out to be of oscillatory character (we note in passing that the critical value of 6.78 is significantly larger than the safe limit of 1.725 for the non-existence of eigenvalues with positive real part, as derived in the previous section, since the latter holds for any $\alpha \in C^1((0,1),\mathbb{R})$). While the oscillation at this value of C is nearly harmonic, a strongly anharmonic oscillation shows up already at the slightly larger value $C = 7.237$ (the similarity of this anharmonic oscillation with the relaxation oscillation of the van-der-Pol oscillator had been discussed in [19]). Increasing C just a little further to $C = 7.24$, this strongly anharmonic oscillation turns into a steady dynamo. For all higher values of C considered here, the dynamo remains steady.

For a few selected values of C, the quenching effect of the self-excited magnetic field on the α profile is illustrated in Fig. 1 (b). Evidently, all initial kinematic profiles α_{kin} with increasing C are quenched into saturated profiles which are actually quite similar in shape and intensity. However, these comparably minor changes of the shape of the profile lead to a drastic change from oscillatory (for $C = 6.8$) to non-oscillatory behaviour (for $C > 7.24$).

Can we understand this saturated dynamo behaviour in terms of spectral theory? In the previous section we learned that in our problem eigenvalues may only form complex conjugate

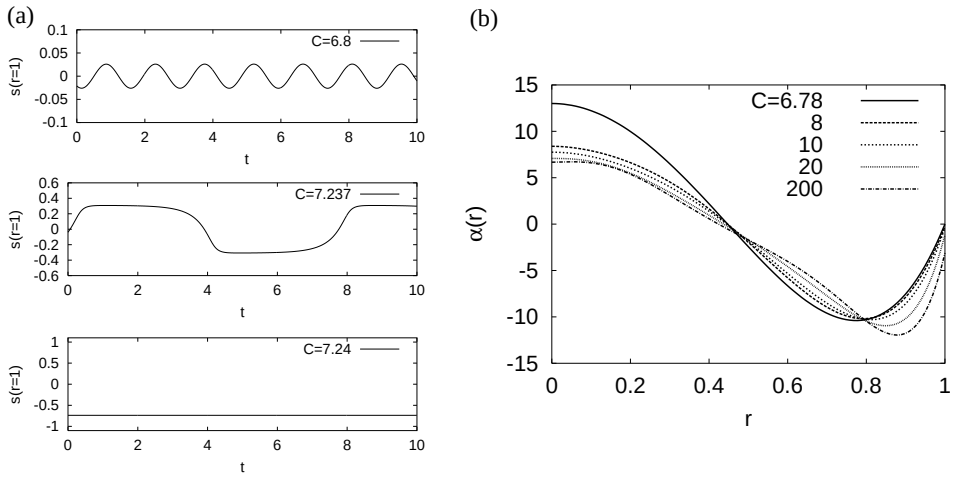

Fig. 1 Typical time series of the α^2 dynamo model for three different values of C (left). With increasing C one observes an increasing degree of anharmonicity which finally turns into a steady state. Right: (nearly) kinematic and four saturated α profiles.

pairs if two real eigenvalues have coalesced at an exceptional point. This is illustrated in Fig. 2 which visualizes the relevant part of the spectrum for four α profiles corresponding to the (nearly) unquenched profile for $C = 6.78$ and to the quenched profiles resulting for $C = 8$, 20 and 200. Note that here the abscissa is labeled by an artificial factor C^* (different from C!) which scales the *quenched* profile (therefore, $C^* = 1$ always corresponds to the point of marginal, saturated dynamo action with zero growth rate, while lower and higher values of C^* just serve to illustrate the spectral behaviour around this point).

These spectra are very telling: while the spectrum for $C = 6.78$ exhibits an exceptional point below the threshold of dynamo action (i.e. for $C^* < 1$), and a complex eigenvalue at $C^* = 1$, the situation changes dramatically for higher values of C. For $C = 8$ the exceptional point has shifted into the right upper part so that for $C^* = 1$ we obtain a non-oscillatory dynamo (see the steady dynamo for $C = 7.24$ as shown in Fig. 1 (a)). Remarkably, for the even higher values $C = 20$ and 200, the exceptional point moves back to a value close to $C^* = 1$. For $C = 200$, it even seems to "cling" to the zero growth rate line, just as if this highly super-critical dynamo would like to develop an exceptional point close to its marginal point. We will come back to this feature further below.

Up to this point, the time evolution was supposed to be completely deterministic which led, depending on the value of C, to (nearly harmonic or anharmonic) oscillations or to steady dynamos. The spectral portraits of Fig. 2 indicate that for high values of C the exceptional point has a tendency to move very close to the marginal point, which makes it likely that even weak noise leads to transitions between non-oscillatory and oscillatory branches. In the following we relate those transitions to the reversals of the (geo-) dynamo field.

This is exemplified in Fig. 3 which shows the time evolution for two values of C, combined with two values of the noise intensity D. Evidently, for $C = 20$ the noise strength $D = 5$ only leads to some fluctuations of the field while it is not sufficient to trigger any reversals. The latter show up, however, for the slightly higher noise level $D = 6$. Interestingly, the stronger

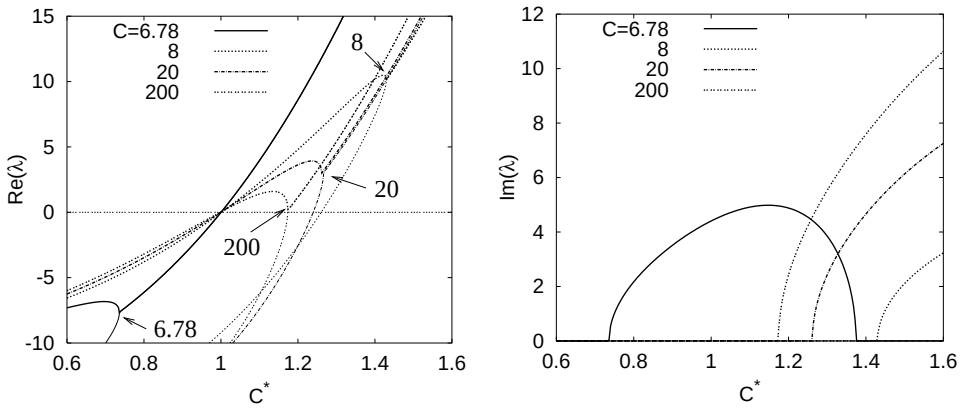

Fig. 2 Spectral properties of the nearly kinematic ($C = 6.78$) and of the saturated (C =8, 20, 200) α profiles which result from the choice $\alpha_{kin}(r) = 1.916 \cdot C \cdot (1 - 6\ r^2 + 5\ r^4)$, $r \in [0, 1]$. The scaling with the artificial factor C^* helps to identify the actual eigenvalue (at $C^* = 1$) in its relative position to the exceptional point. Note that for highly supercritical C the exceptional point moves close to the zero growth rate line. Left: growth rate: Right: angular frequency.

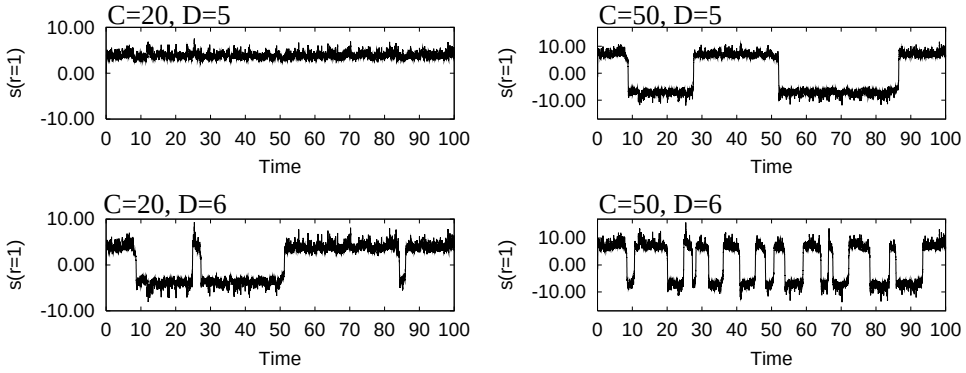

Fig. 3 Time series for various values of C, D and kinematic profile $\alpha_{kin}(r) = 1.916\, C(1-6r^2+5r^4)$.

dynamo with $C = 50$ already exhibits reversals for $D = 5$ which can be attributed to the closer proximity of the exceptional point to the zero growth rate line. For $C = 50$ and $D = 6$, the rate of field reversals becomes quite high.

Fig. 4 provides a schematic explanation of reversals as noise-triggered relaxation oscillations in the vicinity of exceptional points. Actually, this scheme represents a spectral theoretical counterpart of the dynamical systems picture developed in [6] which interprets reversals in terms of a saddle node bifurcation where a pair of a stable and an unstable fixed point is replaced by a Hopf bifurcation. In our Fig. 4, the crossing point S of the real spectral branch with the zero growth rate line represents a stable fixed point for which any slight changes to the left or right would always act in a stabilizing manner. For the unstable fixed point U the situation is different; here, due to the negative slope of the real branch, any change leads to

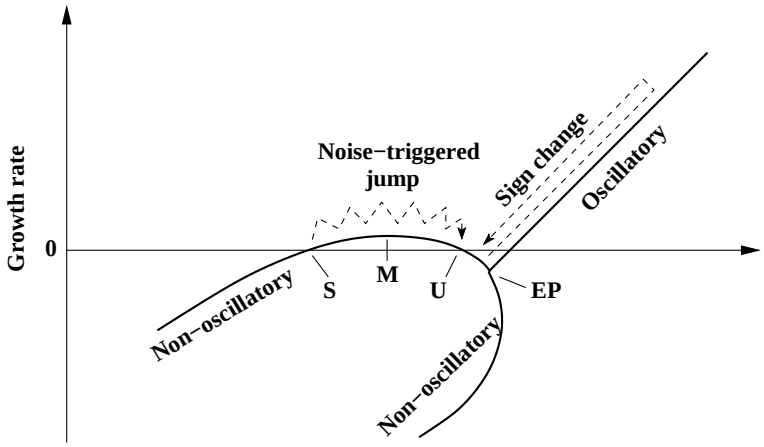

Fig. 4 Illustration of the main mechanism and the various phases of a reversal in the vicinity of an exceptional point of the spectrum of a saturated, highly supercritical dynamo.

a repelling from this point (in close analogy with the van-der-Pol oscillator with its typical "negative differential resistance region"). The role of noise is to bring the system from the stable fixed point S "over the hill" (around the local maximum M) towards the unstable fixed point U, from where it is forced into the oscillatory branch where the very sign change (i.e. where the reversal) occurs, before the system settles again into a stable fixed point.

In Fig. 5 we evidence the remarkable similarity of the reversal process resulting from our model with the typical reversals revealed by paleomagnetic measurements. For the parameter combination $C = 20$, $D = 6$, Fig. 5 (a) exemplifies five typical reversals and their average (note that the time scale has been adjusted to the typical geophysical values). For the sake of comparison, Fig. 5 (b) shows the last five paleomagnetic reversals and their average. Typical for either time series is the well-expressed asymmetry of the reversals, comprising a slow decay and a fast recovery.

In [21] we have pursued this comparison up to the point that we identified (by means of a simplex method) a number of essential parameters of the geodynamo by matching a synthetic reversal process to various paleomagnetic reversal data. In doing so, we have carefully avoided any over-interpretation of our simple model by focusing only on those parameters to be determined, and those functionals to be minimized, that refer to the temporal properties of reversal sequences, and not to any spatial features. This makes us optimistic that the results will prove robust when inversions of this kind will later be repeated using more realistic dynamo models.

5 Conclusions and prospects

In this paper, we have related geomagnetic reversals to the specific spectral properties of non-selfadjoint dynamo operators of mean-field type. For this purpose, we have analyzed in detail the spectra of spherically symmetric α^2 dynamos and have derived strict criteria for the occurrence of complex eigenvalues.

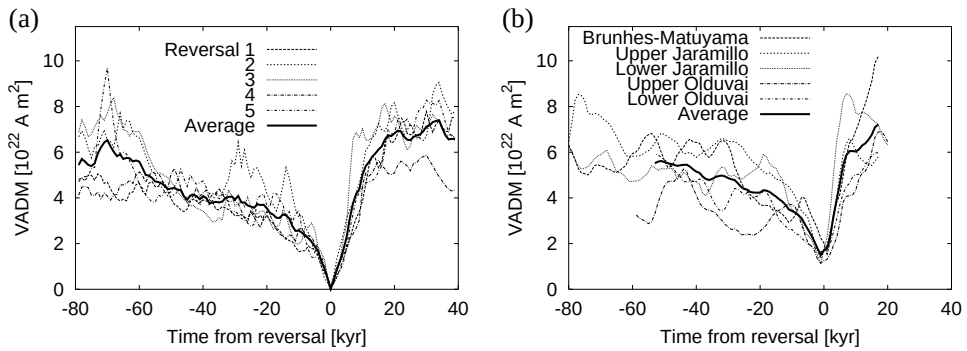

Fig. 5 Comparison of numerically simulated reversals and paleomagnetic reversal data. (a) Five typical reversals resulting from the dynamo model with $\alpha_{kin}(r) = 1.916 \cdot C \cdot (1 - 6\ r^2 + 5\ r^4)$, $r \in [0, 1]$, for $C = 20$, $D = 6$, and their average. The time scale and the scale of the virtual axial dipole moment (VADM) have been chosen in such a way that they become comparable to the geophysical data. Note that the negative VADM values after the reversal have been mirrored to the positive side. (b) VADM during the 80 kyr preceding and the 20 kyr following a polarity transition for five reversals from the last 2 million years (data extracted from [37]), and their average.

Then we have shown that the typical asymmetry of reversals can be explained as a noise triggered relaxation oscillation in the vicinity of an exceptional point of the spectrum where two real branches coalesce to form one common complex branch. While from a purely kinematic viewpoint the occurrence of an exceptional point close to the zero growth rate line appears as rather accidental (and hence of no explanatory use), things are different for the saturated states of highly supercritical dynamos.

For a typical example with a sign change along the radius we have shown that with increasing dynamo strength the modified, saturated α profile develops spectra that become more and more prone to reversals. It is tempting to interpret this mechanism as a sort of self-organized criticality, although more work would be needed to support this claim.

A necessary next step would be to apply our methods to more realistic dynamo models. The three-dimensional structure of α as it results from full 3D simulations of the geodynamo and which also shows the typical sign change along the radius [38, 39] makes this a promising enterprise.

Acknowledgements We thank Uwe Günther for many years of fruitful collaboration on various aspects of the spectral theory of non-selfadjoint operators (F.S.) and the physics of dynamos (C.T.), and for bringing the two authors of this paper together.

References

[1] R.T. Merrill, M.W. McElhinny, and Ph.L. McFadden, The Magnetic Field of the Earth: Paleomagnetism, the Core, and the Deep Mantle, Academic Press, San Diego, 1998.
[2] G.A. Glatzmaier and P.H. Roberts, Nature **377**, 203–209 (1995).
[3] M. Berhanu et al., EPL **77**, 59001 (2007).
[4] F. Stefani, A. Gailitis, and G. Gerbeth, ZAMM **88**, 930-954 (2008).
[5] D. Gubbins, Nature **452**, 165-167 (2008).

[6] F. Pétrélis, S. Fauve, E. Dormy, and J.P. Valet, Phys. Rev. Lett. **102**, 144503 (2009).
[7] E.N. Parker, Astrophys. J. **164**, 491-509 (1971).
[8] W. Deinzer, H.-U. v. Kusserow, and M. Stix, Astron. Astrophys. **36**, 69-78 (1974).
[9] H. Yoshimura, Z. Wang, and F. Wu, Astrophys. J. **283**, 870-878 (1984).
[10] M.L. Dudley and R.W. James, Proc. R. Soc. London A, **425**, 407-429 (1989).
[11] G.R. Sarson and C.A. Jones, Phys. Earth Planet. Inter. **111** (1999) 3-20 (1999).
[12] T. Kato, Perturbation Theory for Linear Operators, Second Edition, Springer Verlag, Berlin. 1976.
[13] U. Günther, F. Stefani, and G. Gerbeth, Czech. J. Phys. **54**, 1075-1089 (2004).
[14] A.P. Seyranian, O.N. Kirillov, and A.A. Mailybaev, J. Phys. A **38**, 1723-1740 (2005).
[15] M.V. Berry and M. Wilkinson, Proc. R. Soc. London A **392**, 15-43 (1984).
[16] F. Stefani and G. Gerbeth, Phys. Rev. E **67**, 027302 (2003).
[17] F. Stefani and G. Gerbeth, Phys. Rev. Lett. **94**, 184506 (2005).
[18] F. Stefani, G. Gerbeth, U. Günther, and M. Xu, Earth Planet. Sci. Lett. **243**, 828-840 (2006).
[19] F. Stefani, M. Xu, L. Sorriso-Valvo, G. Gerbeth, and U. Günther, Geophys. Astrophys. Fluid Dyn. **101**, 227-248 (2007).
[20] L. Sorriso-Valvo, F. Stefani, V. Carbone, G. Nigro, F. Lepreti, A. Vecchio, and P. Veltri, Phys. Earth Planet. Inter. **164**, 197-2017 (2007).
[21] M. Fischer, G. Gerbeth, A. Giesecke, and F. Stefani, Inverse Problems **25**, 065011 (2009).
[22] L.N. Trefethen, M. Embree, Spectra and Pseudospectra. The behavior of nonnormal matrices and operators, Princeton University Press, Princeton, NJ, 2005.
[23] S. Bögli, Integral Equations Operator Theory **88**, 559-599 (2017).
[24] S. Bögli, P. Siegl, C. Tretter, Comm. Partial Differential Equations **42**, 1001–1041 (2017).
[25] U. Günther and F. Stefani, J. Math. Phys. **44**, 3097-3111 (2003).
[26] U. Günther, H. Langer, and C. Tretter, SIAM J. Math. Anal. **42**, 1413-1447 (2010).
[27] A. Giesecke, C. Nore, F. Stefani, G. Gerbeth, J. Léorat, and F. Luddens, Geophys. Astrophys. Fluid Dyn. **104**, 505-529 (2010).
[28] F. Krause and K.-H. Rädler, Mean-field Magnetohydrodynamics and Dynamo Theory, Akademie-Verlag, Berlin, 1980.
[29] J.-C. Cuenin and C. Tretter, J. Math. Anal. Appl. **441**, 235-258 (2016).
[30] C. Tretter, Spectral Theory of Block Operator Matrices and Applications, Imperial College Press, London, 2008.
[31] O.O. Ibrogimov, P. Siegl, and C. Tretter, J. Differential Equations **260**, 3881–3926 (2016).
[32] M. Abramowitz and I.A. Stegun, Handbook of mathematical functions with formulas, graphs, and mathematical tables, National Bureau of Standards Applied Mathematics Series, Washington, D.C., 1964.
[33] H. Langer and C. Tretter, Czech. J. Phys. **54**, 11131120 (2004) and **56**, 10631064 (2006).
[34] Th. Käser, Bachelor thesis, University of Bern, 2017.
[35] S. Bögli, B.M. Brown, M. Marletta, C. Tretter, and M. Wagenhofer, Proc. R. Soc. Lond. A **470**, 20140488, 17 pp. (2014).
[36] B.M. Brown, M. Langer, M. Marletta, C. Tretter, and M. Wagenhofer, LMS J. Comput. Math. **13**, 65-81 (2010).
[37] J.-P. Valet, L. Meynadier, and Y. Guyodo, Nature **435**, 802-805 (2005).
[38] A. Giesecke, U. Ziegler, and G. Rüdiger, Phys. Earth Planet. Inter. **152**, 90-102 (2005).
[39] N. Schaeffer, D. Jault, H.-C. Nataf, and A. Fournier, Geophys. J. Int. **211**, 1-29 (2017).